Journal of Chromatography A, 1218 (2011) 5725–5729

Contents lists available at ScienceDirect

Journal of Chromatography A

journal homepage: www.elsevier.com/locate/chroma

Label-free electrical discrimination of cells at normal, apoptotic and necrotic status with a microfluidic device

Hong-Lei Gou [a], Xian-Bo Zhang [a], Ning Bao [b], Jing-Juan Xu [a,*], Xing-Hua Xia [a], Hong-Yuan Chen [a]

[a] Key Laboratory of Analytical Chemistry for Life Science, School of Chemistry and Chemical Engineering, Nanjing University, Nanjing 210093, China
[b] Institute of Analytical Chemistry for Life Science, School of Public Health, Nantong University, Nantong 226019, China

ARTICLE INFO

Article history:
Received 20 April 2011
Received in revised form 21 June 2011
Accepted 26 June 2011
Available online 3 July 2011

Keywords:
Cell discrimination
Capacitance
Resistance
Microfluidic device

ABSTRACT

As a label-free alternative of conventional flow cytometry, chip-based impedance measurement for single cell analysis has attracted increasing attentions in recent years. In this paper, we designed a T-shape microchannel and fabricated a pair of gold electrodes located horizontally on each side of the microchannel using a transfer printing method. Instant electric signals of flowing-through single cells were then detected by connecting the electrodes to a Keithley resistance and capacitance measurement system. Experimental results based on the simultaneous measurement of resistance and capacitance demonstrated that HL-60 and SMMC-7721 cells could be differentiated effectively. Moreover, SMMC-7721 cells at normal, apoptotic and necrotic status can also be discriminated in the flow. We discussed the possible mechanism for the discrimination of cell size and cell status by electrical analysis, and it is believed that the improvement of detection with our design results from more uniform distribution of the electric field. This microfluidic design may potentially become a promising approach for the label-free cell sorting and screening.

1. Introduction

It is of great significance in diagnostic and research applications for high throughput and fast analysis of single cells, which is represented by flow cytometry. In conventional flow cytometry, single cells could be analyzed according to the distributions of fluorescent signals from labeled cells induced by a laser beam [1,2]. However, the fluorescent labeling procedure for the samples may induce harassment and alteration to the studied system. The electrical properties of biological cells have been studied for a long time [3–6]. Cellular electrical properties play critical roles in the physiology of living cells. As a nondestructive and label-free analytical tool, impedance spectroscopy has been used to measure the passive electrical properties of biological cells for many years, both in bulk suspensions [7–9] and on substrates [10–13]. To date, the Coulter counter is the first successful device for measuring the electrical properties of single particles and single cells [14]. It employs two electrically isolated fluid-filled chambers connecting with a small aperture to measure the resistance at DC voltage or the impedance at low frequency AC voltage, which is depended upon the cell volume.

In recent years, microfluidic devices have been widely applied for cell analysis due to their dimensions comparable to single cells [15–18]. Particularly, flow impedance measurements based on the dielectric properties of cells have been developed [19–22]. A simple design is the micro-Coulter counter, which measures the impedance signals as the cells passing through, by using a pair of electrodes fabricated either opposite on the channel wall or coplanar at the channel bottom [23–27]. Another approach, named the single cell impedance cytometry [28–36], applies multiple discrete frequencies of AC voltage to measure the impedance of mobile cells. In this case, one or two pairs of parallel overlapped electrodes are integrated for excitation and detection, respectively. Additionally, capacitance cytometry [37] and resistive pulse sensing technique [38] have also been developed for measuring DNA content and cell counting. However, based on the impedance measurement of single cells, few reports refer to the differentiation of cells at normal, apoptotic and necrotic status in microfluidic systems. Since the cell status is essential for biological studies on cells, it is necessary to develop a rapid and label-free approach for its identification and discrimination over the traditional ways [39,40].

In this paper, we present a simple design of a microfluidic device for the discrimination of flowing cells, which contains a T-shape microchannel and two on-chip electrodes based on the chemical plating and transfer printing methods [41,42]. With such a design, we were able to measure both the capacitance and resistance of the flowing single cells simultaneously. Moreover, with our device

* Corresponding author. Tel.: +86 25 83594862; fax: +86 25 83594862.
E-mail address: xujj@nju.edu.cn (J.-J. Xu).

0021-9673/$ – see front matter © 2011 Elsevier B.V. All rights reserved.
doi:10.1016/j.chroma.2011.06.102

discrimination of cells of different sizes as well as cells at normal, apoptotic and necrotic status could be effectively performed.

2. Experimental

2.1. Materials and reagents

Sylgard 184 (including PDMS monomer and curing agent) was purchased from Dow Corning (Midland, MI). Acridine Orange (AO) and ethidium bromide (1%, w/v, EB) was from Amresco (Solon, OH). Fluorescein isothiocyanate isomer (FITC) and 3-aminophenylboronic acid monohydrate (APBA) were from Sigma (St. Louis, MO). Glucose and mannitol was from Shanghai Bio Life Science & Technology Co., Ltd. (Shanghai, China). All other chemicals were of analytical grade and used without further purification. Milli-Q grade water (Millipore Inc., Bedford, MA) was used for all solutions and cleaning steps. The buffer was 10 mM phosphate-buffered saline (PBS, pH 7.4) containing 137 mM NaCl, 2.7 mM KCl, 87.2 mM Na_2HPO_4 and 14.1 mM KH_2PO_4. Detection solution was an isotonic buffer solution (pH 7.4) containing 250 mM mannitol, 10 mM HEPES, 15 mM K_3PO_4, and 1 mM $MgCl_2$.

2.2. Cell lines and sample preparation

Human liver carcinoma (SMMC-7721) and Human promyelocytic leukemia cells (HL-60) were obtained from Gulou Hospital (Nanjing, China). For ordinary culture, they were maintained in Dulbecco's Modified Eagle Media (DMEM, Gibco Invitrogen Corp., USA) supplemented with 10% fetal bovine serum (Gibco Invitrogen Corp., USA) at 37 °C and 5% CO_2 environment. Confluent HL-60 cell and pre-trypsinized SMMC-7721 cells were both washed and then resuspended in the detection solution at a density of ca. 5×10^5 cells mL^{-1} before used. Cells at different status were obtained using SMMC-7721 cell line. Cells at logarithmic phase for keeping normally cultured for 6 h were collected, washed and suspended in detection solution as the normal cells. Apoptotic cells were harvested with 8% ethanol in complete medium for 6 h, and necrotic cells were obtained by treating normal cells with 95% ethanol for 1 h. All the cells at three kinds of stage were suspended in detection solution at a density of ca. 5×10^5 cells mL^{-1} before use.

Fluorescence staining with AO, EB and self-synthesized FITC labeled APBA (FITC-APBA) were used for fluorescence observation of normal living cells, necrotic cells and apoptotic cells, respectively, to provide evidential relationships between flowing cells and corresponding electrical signals (see supporting information).

2.3. Device set-up

By gold chemical plating and transfer printing method developed by our group previously [41,42], gold coated area was fabricated on a base PDMS layer surface orthogonally with the microchannel (60 μm wide and 30 μm deep), which separated the gold band into two parts oppositely molding on both sides along the channel. Besides, a PDMS slice with a 200 μm width and 5 μm depth channel was fabricated as a cover layer by a master printed with a laser printer [43]. Both layers were then simultaneously treated with air plasma to form hydrophilic surfaces. After that, the two PDMS layers were combined together with the upper channel right above aligning the base channel. Drying for an hour under infrared lamp, the two layers were compactly adhered to each other. Because the upper channel was wider than the base one, a small part of the gold electrodes about 70 μm × 150 μm was exposed to form opposite pairs of microelectrodes on each side along the T-shape channel. Areas of the gold outside the cover layer were made into pads of the electrodes and led out to the data acquisition system. The whole procedure is shown in Fig. 1.

2.4. Instruments and softwares

DMIRE2 Inverted fluorescence microscope (Leica, Germany) equipped with DP71 CCD (Olympus, Japan) and Image-Pro Plus (IPP) software were used for micro-imaging and video previewing (bright-field and fluorescent images). Photos were taken by using a Nikon camera 4300. The measurements of capacitance and resistance were performed with a Keithley 4200-SCS semiconductor characterization system (OH, USA) with a CVU module. COMSOL Multiphysics (version 3.3) was used to simulate the electric field distribution between the two electrodes. A free screen recording software (Camtasia Studio, V5.0) was employed to obtain and combine the videos and snapshots for cells flowing through the electrodes gap and corresponding synchronous signals.

2.5. Cell loading and measurements

Homogeneous cells or mixed cells suspended in detection solution were loaded into the inlet of the chip, adjusting the flowing rate of the cells by hydrostatic stress to make them move one by one into the detection area. A small AC voltage at 100 kHz with amplitude of 100 mV with a DC bias voltage of 0 V was applied to the detection system to measure the capacitance and resistance between a pair of electrodes in a low conductive mannitol isotonic solution. The values of capacitance and resistance of cells were measured simultaneously with Keithley 4200-SCS during a single cell passing through the narrow detection area. The experiments

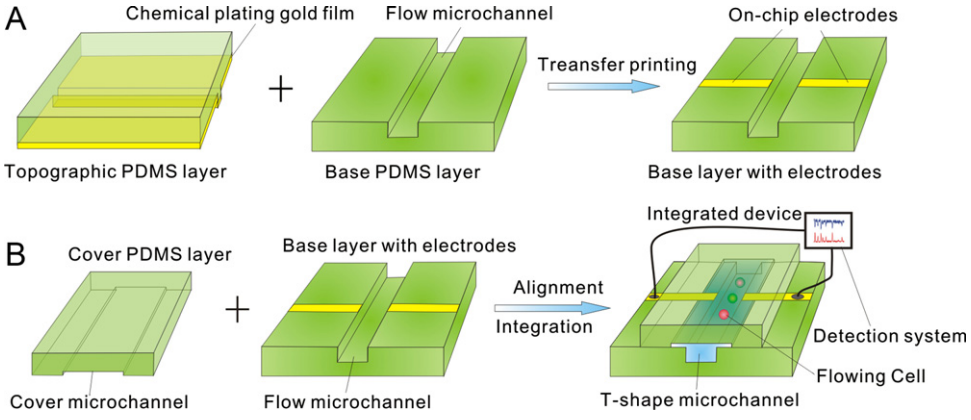

Fig. 1. Fabrication process of the on-chip electrodes (A) and the integrated device (B).

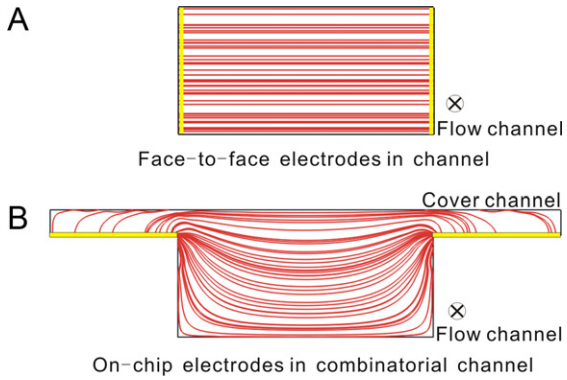

Fig. 2. Simulation of the distribution of the electric field in different designs of on-chip electrodes. (A) Face-to-face electrodes in channel, cross section view of the channel; (B) on-chip electrodes in T-shape channel for our design, cross section view of the channel.

were carried out at room temperature. Data acquisition and video recording under a fluorescent mode were started at the same time.

3. Results and discussion

3.1. Design and principle

Previous study revealed that the structure of the on-chip electrodes may greatly affect the impedance measurement. The configuration of co-planar electrodes in the microfluidic system is simple and has been extensively studied and reported for electric detection of cells [25–27]. To the best of our knowledge, however, the differentiation of cells at normal, apoptotic and necrotic status has not been reported with such a design. It was suggested that the geometry of face-to-face electrodes on the opposite sides of the channel might be more suitable for the impedance measurement of single cells than the common co-planar electrodes [28]. However, because of complicated fabrication process it is difficult to apply the face-to-face electrodes in the microchannel even using the advanced microfabrication techniques. To address this problem, here we integrated a T-shape channel structure with a pair of on-chip electrodes. The T-shape microchannel was obtained using two microfluidic chips consists of a microchannel with different widths (Fig. 1). By transfer printing [42], a pair of gold microband electrodes was fabricated horizontally on each side of the narrower microfluidic channel.

We simulated the electric flux in different designs of on-chip electrodes with COMSOL. As shown in Fig. 2A, the electric flux of face-to-face mode is quite uniform across the microchannel, which possibly leads to a sensitive electrical response when the cell is flowing through. By comparison, in our design (Fig. 2B) the electric flux is across the microchannel and similar to that of the face-to-face design. In the middle of the channel the electric flux is close to uniform. Based on the above simulation, the designed chip is further investigated on the measurement of cells at different sizes and status.

In the following the equivalent circuits between the two electrodes were analyzed both with and without a cell. It has been suggested that the cell membrane could be regarded as a significant barrier to the current flow and be essentially non-conducting under the applied DC or AC electric field with low frequencies (up to 1 MHz) [20,22,44]. In this case, the cell could be presented as a uniform and spherical conductive cytoplasm surrounded by a thin non-conductive membrane. When a cell is flowing between the two electrodes, its equivalent circuit model can be described in Fig. 3A [20,22,35]. The resistance and capacitance of the fluid surrounding the cell originated from the buffer solution. In our investigation, we

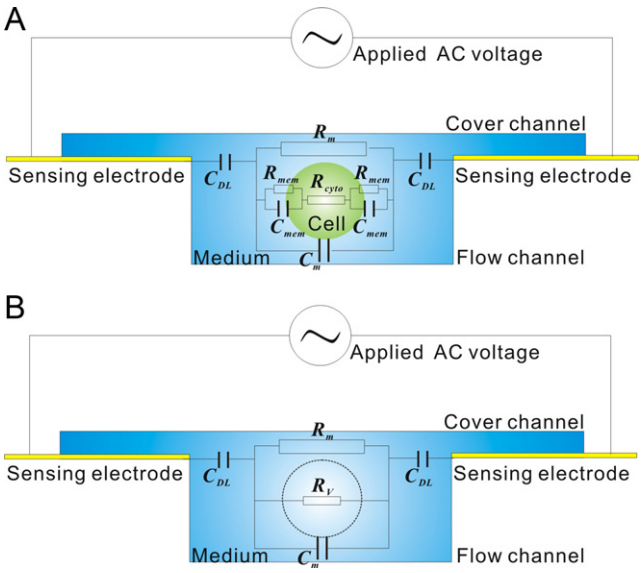

Fig. 3. Schematic diagrams of equivalent circuit in detection area with (A) and without (B) a suspended cell but a dummy volume which is shown with dashed line. Here, C_{DL} represents the capacitance of the electrical double layers, R_m and C_m the resistance and capacitance of the medium, R_{mem} and C_{mem} the resistance and capacitance of the cell membrane and R_{cyto} the resistance of the cytoplasm, R_V is the resistance of the expelled volume of medium by a single cell to be detected.

hypothesized that the cell membrane could be represented using a capacitor (C_{mem}) in parallel with a resistor (R_{mem}) and its cytoplasm by a resistor (R_{cyto}) in series in order to simplify the circuit. The medium surrounding the cell could then be represented with two elements (R_m and C_m) in parallel to the cell according to the direction of the electric flux. At the electrode–solution interface, capacitance of the electrical double layer due to the electrode polarization could be generally modeled as a capacitor (C_{DL}) in series. Generally speaking, it would introduce negative influences to the electrochemical detection at a low frequency of below 100 kHz for high conductivity solutions, such as PBS [45]. In our experiments, the working medium of mannitol isotonic buffer solution with lower conductivity was employed. Because of this low conductivity, it is believed that the charge intensity on the surface of the electrode is low enough so that the capacitance of the double layer could be neglected with the AC frequency of 100 kHz. By comparison, Fig. 3B shows the equivalent circuit between two electrodes without a cell. In order to simplify the circuit, here R_V was used to represent the resistance of the expelled medium whose volume is corresponding to that a single cell. Thus the total resistance for the medium is $R_V + R_m$.

The possible detection mechanism was then studied according to the simulated electric flux in Fig. 2B. As a cell passes through this area, it displaces the same volume of conductive solution and alters the electric flux so that the current will be changed. Meanwhile, the biological cell is polarized under the applied AC electric field at the low frequency because of the accumulation of charges at the boundaries between the thin insulating membrane and the aqueous suspending medium with different dielectric properties. When a cell is in between the two on-chip electrodes, the resistance and capacitance would be changed due to the replacement of a corresponding volume of medium by the cell which has heterogeneous electrical properties. It has been reported that for a single cell, the capacitance is mainly resulted from the cell membrane and the resistance mainly from the cell cytoplasm [20,21]. In this case, the membrane resistance and cytoplasm capacitance could be largely neglected. In our design, the Keithley system with a CVU module, including a signal generator and a response detector, could

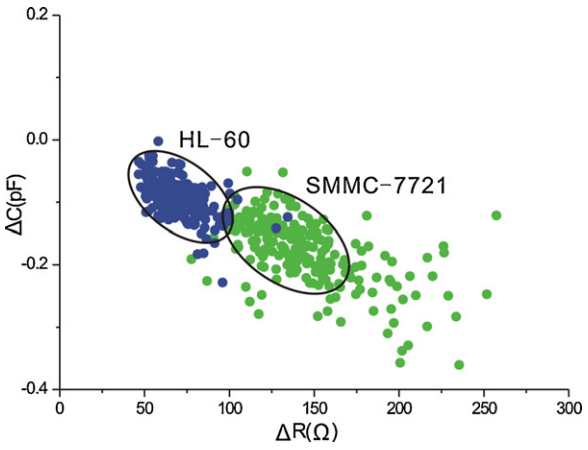

Fig. 4. Scatter plot of capacitance and resistance changes for HL-60 and SMMC-7721 cells.

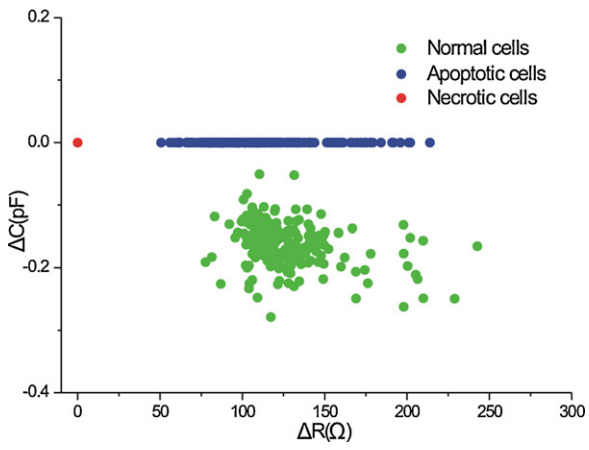

Fig. 5. Scatter plot of capacitance and resistance changes for normal, apoptotic and necrotic SMMC-7721 cells.

simultaneously measure the capacitance and resistance between two on chip electrodes at a certain AC frequency. Thus, the resistance and capacitance could be obtained to reflect the difference of individual cells on cytoplasm and membrane, etc., so that our design could be used for discrimination of cells with different sizes and different cell status.

3.2. Discrimination of cells with different sizes

Fig. 4 shows the scatter plots of measured capacitance and resistance response for HL-60 cells and SMMC-7721 cells with our approach separately. It could be observed from the scatter plots that data distributions of two cell types located mainly in two discernable areas. Most HL-60 cells have lower resistance and lower capacitance while SMMC-7721 cells have higher resistance and higher capacitance. The scattered points out of these two areas were possibly from the multi-cells. Those cells are so close when they were flowing through the sensing area that they could not be detected separately (see Figs. S1 and S2 in supporting information). Table 1 statistically compares the measured results of resistance and capacitance with the corresponding cell sizes. It could be found that both cells have very close values of $\overline{\Delta R}/\overline{\text{Size}}$ and $-\overline{\Delta C}/\overline{\text{Size}}$ although they have different sizes, which might be a reflection of intrinsic electrical properties of biological cells. Our data revealed that the discrimination of cells with different sizes could be achieved based on the measurement of capacitance and resistance with our design (see Fig S3, which shows the raw data of capacitance and resistance signals from a mixture sample of HL-60 and SMMC-7721 cells). Because our approach is nondestructive to cells, it may potentially be applied for cell sorting. However, the separation of different types of cells may only be performed after establishment of related database on electric detection of cells.

3.3. Discrimination of cells at normal, apoptotic and necrotic status

Fig. 5 shows the measurements of resistance and capacitance on the SMMC-7721 cells at normal, apoptotic and necrotic status (some raw data are shown in Fig. S4 in supporting information). It could be observed that the distribution of capacitance and resistance of the cells at normal status located in the similar area to that shown in Fig. 4. Interestingly, for the cells at apoptotic status the distribution of resistance shifted a little while that of capacitance located at zero. For the cells at necrotic status, the resistance and capacitance changes were measured to be zero so that both their distributions located at zero for a point. Our results were different comparing with previous report, in which dead and viable cells could be distinguished by impedance measurements at AC frequency of 4 MHz using two pairs of parallel overlapped electrodes, and with the increase of frequency to 6 MHz, necrotic from apoptotic cells could be discriminated with sufficient resolution [44]. While in our work, normal, apoptotic and necrotic cells could be effectively distinguished at 100 kHz. The reason of the difference might be attributed to the different electrode structure and measurement approach, which detected both the capacitance and resistance of cells simultaneously in our work. The differentiation of cells at normal, apoptotic and necrotic status with our approach makes it possible for label-free cell sorting.

The differences of resistance and capacitance between the cells at three statuses might result from the changes of cell membrane and cytoplasm according to previous reports [32,46–48]. Normal living cells have intact membrane, natural morphology and interior components of cytoplasm. Thus, they have the biggest dielectric difference compared with the medium so that the changes on resistance and capacitance are remarkable. When the cells are induced to be apoptosis, the cell membrane and cytoplasm are both changed [49,50]. For the membrane of a cell at apoptotic status, the movement of phospholipids caused a randomization of the lipid distribution and the externalization of phosphatidylserine, accompanied with the structure changes such as micro-villi, folds and blebs. Therefore, the conductivity and permittivity of the membrane were both changed. The membrane capacitance C_{mem} decreased so that the capacitance response of the cell was measured to be zero. Meanwhile in the cytoplasm, resistance R_{cyto} also decreased because of the volume condensation, the chromatin aggregation and the DNA fragmentation, etc. While the plasma membrane still kept intact that it holded on the barrier to the electric field, lower resistance responses remained but capacitance

Table 1
The results of measurements for HL-60 and SMMC-7721 cells.

Type of cells	Size of cell (μm)	ΔR (Ω) measured	$-\Delta C$ (pF) measured	Average size (μm)	$\overline{\Delta R}$ (Ω) measured	$-\overline{\Delta C}$ (pF) measured	$\overline{\Delta R}/\overline{\text{Size}}$ (Ω/μm)	$-\overline{\Delta C}/\overline{\text{Size}}$ (pF/μm)
HL-60	8–15	50–100	0.05–0.15	11.5	75	0.10	6.52	8.7×10^{-3}
SMMC-7721	15–25	90–170	0.10–0.25	20	130	0.175	6.50	8.8×10^{-3}

signals disappeared. For necrotic cells, the membrane became permeable and the cytoplasm spilled out so that the membrane of dead cell was hardly polarized and holding no barrier to the electric field any more. As a result, both R_{cyto} and C_{mem} were eliminated so that both capacitance and resistance signals disappeared.

3.4. Verification of different electrical responses

It has been reported that the fluidity of cell membrane could be changed through the treatment of many polymer chemicals, such as polyethylene glycol (PEG), polyvinyl alcohol (PVA), polyvinylpyrrolidone (PVP) and polyglycerine. As a result, phospholipids would be redistributed without influence on the cytoplasm, which is the basis for cell chemical fusion [51,52]. Based on the circuit model, in this case, C_{mem} was changed while R_{cyto} was basically not affected, so that resistance would keep similar while capacitance would be changed. After treated with 2% PVA for 30 min, the resistance responses of most cells changed a little but the capacitance values decreased to be zero (see Fig. S5 in supporting information). Such results demonstrated that the capacitance of a living cell is only determined by the properties of the cell membrane. Moreover it could be used to explain why the apoptotic cells only have resistance response but no capacitance signals.

4. Conclusions

By applying a simple design, we successfully constructed a microfluidic device for the effective discrimination of flowing single cells at normal, apoptotic and necrotic status. This approach employed a T-shape microchannel structure and a pair of on-chip gold electrodes. Cells were analyzed based on the simultaneous measurements of capacitance and resistance. Our experimental data demonstrated that this approach could be successfully applied for the analysis of cells with different sizes as well as cells at normal, apoptotic and necrotic status. This study suggested that by employing new electrodes structure, the impedance measurements with simultaneous acquisition of resistance and capacitance could improve the discrimination of normal, apoptotic and necrotic cell status. Our approach could be improved by employing fine electrodes, hydrodynamic focusing and fast data acquisition. With these improvements, it could not only be potentially applied for electrical flow cytometry but also make it possible for the development of label-free sorting of cells based on electrical measurements.

Acknowledgements

This work was supported by the National Natural Science Foundation of China (20890021, 21075070), the National Natural Science Funds for Creative Research Groups (20821063), and the 973 Program (2007CB936404, 2006CB933201). And the authors appreciate the assistance in COMSOL stimulation from Dr. Zengqiang Wu.

Appendix A. Supplementary data

Supplementary data associated with this article can be found, in the online version, at doi:10.1016/j.chroma.2011.06.102.

References

[1] H.M. Daveyn, D.B. Kell, Microbiol. Rev. 60 (1996) 641.
[2] H.M. Shapiro, Cytometry A 58A (2004) 3.
[3] K.R. Foster, H.P. Schwan, Crit. Rev. Biomed. Eng. 17 (1989) 25.
[4] X. Cheng, Y. Liu, D. Irimia, U. Demirci, L. Yang, L. Zamir, W. Rodríguez, M. Toner, R. Bashir, Lab Chip 7 (2007) 746.
[5] S.Z. Hua, T. Pennell, Lab Chip 9 (2009) 251.
[6] R. de la Rica, S. Thomson, A. Baldi, C. Fernandez-Sanchez, C.M. Drain, H. Matsui, Anal. Chem. 81 (2009) 10167.
[7] H.M. Davey, C.L. Davey, A.M. Woodward, A.N. Edmonds, A.W. Lee, D.B. Kell, Biosystems 39 (1996) 43.
[8] G. Fuhr, H. Glasser, T. Muller, T. Schnelle, Biochim. Biophys. Acta 1201 (1994) 353.
[9] R. Lisin, B.Z. Ginzburg, M. Schlesinger, Y. Feldman, Biochim. Biophys. Acta 1280 (1996) 34.
[10] J.H.T. Luong, C. Xiao, B. Lachance, S.M. Leabu, X. Li, E. Al, Anal. Chim. Acta 501 (2004) 61.
[11] C. Xiao, B. Lachance, G. Sunahara, J.H. Luong, Anal. Chem. 74 (2002) 1333.
[12] L. Ceriotti, J. Ponti, P. Colpo, E. Sabbioni, F. Rossi, Biosens. Bioelectron. 22 (2007) 3057.
[13] P. Linderholm, T. Braschler, J. Vannod, Y. Barrandon, M. Brouard, P. Renaud, Lab Chip 6 (2006) 1155.
[14] W.H. Coulter, Proc. Nat. Electron. Conf. 12 (1956) 1034.
[15] N. Bao, J. Wang, C. Lu, Anal. Bioanal. Chem. 391 (2008) 933.
[16] A.K. Price, C.T. Culbertson, Anal. Chem. 79 (2007) 2614.
[17] T.C. Chao, A. Ros, J.R. Soc, Interface 5 (2008) S139.
[18] G.B. Salieb-Beugelaar, G. Simone, A. Arora, A. Philippi, A. Manz, Anal. Chem. 82 (2010) 4848.
[19] H.P. Zhang, C.H. Chon, X.X. Pan, D.Q. Li, Microfluid Nanofluid 7 (2009) 739.
[20] H. Morgan, T. Sun, D. Holmes, S. Gawad, N.G. Green, J. Phys. D: Appl. Phys. 40 (2007) 61.
[21] T. Sun, D. Holmes, Microfluid Nanofluid 8 (2010) 423.
[22] K. Cheung, S. Gawad, Ph. Renaud, Cytometry A 65A (2005) 124.
[23] M. Koch, A.G.R. Evans, A. Brunnschweiler, J. Micromech. Microeng. 9 (1999) 159.
[24] H. Chun, T.D. Chung, H.C. Kim, Anal. Chem. 77 (2005) 2490.
[25] R. Rodriguez-Trujillo, O. Castillo-Fernandez, M. Garrido, M. Arundell, A. Valencia, G. Gomila, Biosens. Bioelectron. 24 (2008) 290.
[26] N. Watkins, B.M. Venkatesan, M. Toner, W. Rodriguez, R. Bashir, Lab Chip 9 (2009) 3177.
[27] L.I. Segerink, A.J. Sprenkels, P.M. ter Braak, I. Vermes, A. van den Berg, Lab Chip 10 (2010) 1018.
[28] S. Gawad, L. Schild, Ph. Renaud, Lab Chip 1 (2001) 76.
[29] T. Sun, D. Holmes, S. Gawad, N.G. Green, H. Morgan, Lab Chip 7 (2007) 1034.
[30] T. Sun, S. Gawad, N.G. Green, H. Morgan, Meas. Sci. Technol. 18 (2007) 2859.
[31] S. Gawad, T. Sun, N.G. Green, H. Morgan, Rev. Sci. Instrum. 78 (2007) 054301.
[32] G. Schade-Kampmann, A. Huwiler, M. Hebeisen, T. Hessler, M. Di Berardino, Cell Prolif. 41 (2008) 830.
[33] T. Sun, C. van Berkel, N.G. Green, H. Morgan, Microfluid Nanofluid 6 (2009) 179.
[34] D. Malleo, J.T. Nevill, L.P. Lee, H. Morgan, Microfluid Nanofluid 9 (2010) 191.
[35] D. Holmes, D. Pettigrew, C.H. Reccius, J.D. Gwyer, C. van Berkel, J. Holloway, D.E. Davies, H. Morgan, Lab Chip 9 (2009) 2881.
[36] D. Holmes, H. Morgan, Anal. Chem. 82 (2010) 1455.
[37] L.L. Sohn, O.A. Saleh, G.R. Facer, A.J. Beavis, R.S. Allan, D.A. Notterman, Proc. Natl. Acad. Sci. U.S.A. 97 (2000) 10687.
[38] X.D. Wu, C.H. Chon, Y.N. Wang, Y.J. Kang, D.Q. Li, Lab Chip 8 (2008) 1943.
[39] M.M. Michelle, D.R. Randall, P. Dimitri, Anal. Methods 2 (2010) 996.
[40] D.V. Krysko, T. Vanden Berghe, K. D'Herde, P. Vandenabeele, Methods 44 (2008) 205.
[41] H.J. Bai, M.L. Shao, H.L. Gou, J.J. Xu, H.Y. Chen, Langmuir 25 (2009) 10402.
[42] H.L. Gou, J.J. Xu, X.H. Xia, H.Y. Chen, ACS Appl. Mater. Interfaces 2 (2010) 1324.
[43] N. Bao, Q. Zhang, J.J. Xu, H.Y. Chen, J. Chromatogr. A 1089 (2005) 270.
[44] A. Pierzchalski, M. Hebeisen, A. Mittag, M. di Berardino, A. Tarnok, Proc. SPIE 7568 (2010) 75681B.
[45] F. Bordi, C. Cametti, T. Gili, Bioelectrochemistry 54 (2001) 53.
[46] J. Yang, Y. Huang, X.J. Wang, F.F. Becker, P.R.C. Gascoyne, Biophys. J. 76 (1999) 3307.
[47] X. Wang, F.F. Becker, P.R.C. Gascoyne, Biochim. Biophys. Acta 1564 (2002) 412.
[48] K. Ratanachoo, P.R.C. Gascoyne, M. Ruchirawat, Biochim. Biophys. Acta 1564 (2002) 449.
[49] Z. Darzynkiewicz, G. Juan, X. Li, W. Gorczyca, T. Murakami, F. Traganos, Cytometry 27 (1997) 1.
[50] M.O. Hengartner, Nature 407 (2000) 770.
[51] I. Karube, E. Tamiya, H. Matsuoka, FEBS Lett. 175 (1984) 13.
[52] J.K. Lee, B.R. Lentz, Biochemistry 36 (1997) 6251.